INSTITUTE OF HIGH ENERGY PHYSICS, SERPUKHOV

Report IFVE OP 70-98

CHANNEL SYSTEM FOR NEGATIVE PARTICLES WITH A MOMENTUM OF UP TO 40 GeV/c

M.I. Grachev, K.I. Gubrienko, E.V. Eremenko, V.P. Kartashev,
V.I. Kotov, A.V. Samojlov, V.S. Seleznev and Yu.S. Khodyrev

Serpukhov 1970

Translated at CERN by B. Hodge
(Original: Russian)
Revised by N. Mouravieff

(CERN Trans. 72-12)

Geneva
June 1972

The channels examined below were constructed on the IHEP accelerator and intended for forming beams of secondary negative particles in the 25-40 GeV/c momentum range, for an accelerated proton energy of 70 GeV. Figure 1 shows the arrangement of the channels in the experimental hall. They consist of standard channel components (quadrupole lenses, bending magnets, remote-controlled collimators etc.) designed by the D.V. Efremov Scientific Research Institute of Experimental Physics Apparatus. The principal characteristics of the equipment and the design of the channels have been examined in papers /1-3/. The channels (4A, 4B and 4C) share a common initial section, including a target station, and form a single complex. Each channel can be operated with different optical arrangements depending on the layout of the particular experiment. Channel 4A has been used for studies of the yields of π^-, K^- - mesons, antiprotons and anti-deuterons and an experiment is now being carried out to study charge exchange processes; on channel 4B, equipment has been set up to study back-scattering processes and a 2 metre bubble chamber has been installed; channel 4C is being used for an experiment to track down heavy particles and contains a boson spectrometer, which has recently started operation. Such an extensive programme of experiments, imposing widely differing requirements in respect of the parameters of the beams formed, involves a high degree of versatility when re-adapting the channels to new operating modes.

The optical layouts of this complex are shown in figure 2. The secondary particles are produced on three internal targets situated in the second section of the 27th magnet unit. The number and location of the targets was determined by the requirement that the extraction of secondary particles into the channel should be effected with the smallest possible production angles on the targets, in the widest possible momentum range for a fixed energy of the accelerated protons (see figure 3a). The secondary particle momentum can be varied by choosing the appropriate target and adjusting its radial position within $\pm$ 4 cm with respect to the equilibrium orbit.

Particles with momenta of 40; 31.6 and 25 GeV/c then have zero production angles on targets 1, 2 and 3 respectively.

The influence of the accelerator's magnetic field on the secondary particle beam's linear and angular characteristics is illustrated in the graphs of figures 3b and 4; these show, depending on the particle momentum, the variation in the position of imaginary sources, in the linear magnification coefficients and linear dispersion of an imaginary source according to the momentum.

At the accelerator exit the particle beam is trimmed by vertical and horizontal **aperture collimators**, C1 and C2 (see Figure 2). A quadrupole lens doublet, Q1 and Q2, with DF focusing (defocusing/focusing) in the horizontal plane forms an image in the centre of a **momentum collimator, C4 or C5, according to the channel.** Vertically, focusing is essentially independent of the subsequent optical system and is determined by the requirement that the angle of particle capture in the channel must be the largest possible. The bending magnet M1, which allows for the influence of the accelerator's magnetic field, provides a dispersion on the **momentum** collimators C4 and C5 of 7 mm and 10 mm respectively for 1 % $\frac{\Delta p}{p_o}$ (Δ p is the deviation of the particle's momentum in relation to the central momentum p_o). The subsequent optical channel lay-outs are substantially different from each other, and we shall examine them separately.

Channel 4A. After a momentum analysis, the beam is deflected away from the accelerator by magnet M2 (see Figure 2a). The Q4, Q5 quadrupole lens doublet with FD focusing in the horizontal plane forms a parallel beam in both transverse directions or focuses it onto an experimental set-up. To produce the parallel beam the **momentum** collimator C5 is used. In the second case, the **momentum collimator** used is C4, because when collimator C5 is used the Q4, Q5 lens doublet is not powerful enough to focus the beam onto the experimental set-up.

Channel 4B. The optical system of this channel is achromatic (see Figure 2b). A field lens Q 3, located behind the momentum collimator C4, operating in conjunction with the bending magnet M3 (in this case magnet M2 is switched off), compensates the linear and angular dispersion. The Q6, Q7 lens doublet, which has FD focusing in the horizontal plane operates in two modes.

When studying the back-scattering processes, the Q6, Q7 lens doublet focuses the particle beam on to a hydrogen target in front of magnet M4, which is part of the experimental set-up and serves, at the same time, as a distributing magnet. When the bubble chamber is being operated the Q6, Q7 lens doublet focuses the particles horizontally and vertically into collimators C6 and C7 respectively. These intermediate images serve as sources for the following lens unit Q6, Q9 which forms the beam prior to entry into the chamber.

Channel 4C. In the complex we are considering, the channel which is most densely packed with optical equipment is 4C (see figure 2c). Structurally, it consists of two achromatic systems, similar to that used in channel 4B. The field lens Q3 located behind the momentum collimator C4, operating in conjunction with the bending magnet M2, compensates the linear and angular dispersion. The Q10, Q11 quadrupole lens doublet, which has horizontal FD focusing, converts the beam in both transverse planes into one which is parallel. The beam divergence over this section, which is intended for the installation of a differential Čerenkov counter does not exceed $\pm$ 0.5 mrad when $\frac{\Delta p}{p_o} = \pm 1\ \%$ (see Figure 5b). The subsequent optical system of the channel is a mirror image of the first half already described. The final lens doublet, (Q15, Q16) of the second achromatic system focuses the beam onto an experimental set-up 30 or 18 metres away, depending on the experiment concerned. In the second case, unlike the first, the final lens unit operates in the DF mode in the horizontal plane.

Calculation of the secondary particle beam characteristics

and the optical layouts of all three channels was by means of computers using standard programmes prepared by the IHEP[4,5]. Figure 5 shows the phase characteristics of the beams on the parallel channel sections 4A and 4C respectively. Curves representing the solid angle of particle capture in the channels and the momentum resolution are shown in figure 6. The momentum resolution value $\frac{\Delta p}{p_o}$ was taken at level of 0.1 Ω_{max}. As figure 6 shows, the maximum solid angles of particle capture in channels 4A, 4B and 4C are 36, 18 and 30 microsteradians respectively. Limitation of the solid angle of capture in channel 4B was the result of using small-aperture 10 cm diameter quadrupole lenses (Q6 - Q9, shown in Figure 2b). The operating modes of the channels were investigated in the same sequence as that for the channel of negative particles of 40 - 60 GeV/c [1]. The channels were tuned by using virtually all the familiar methods (see, for example, /6/), although some were modified to shorten the tuning time. We shall not give a detailed description of the whole sequence of tuning procedures, but mention only the most typical of these.

The total particle flux in the channels was measured with three scintillation counters, 20 cm in diameter and 1 cm thick, connected to work in coincidence. Instead of pencil-type counters for determining the profile and position of the beam in the vertical and horizontal planes, point-type counters measuring 1 x 1 x 1 cm were used. These were fixed to remote-controlled frames which enabled them to be moved over the beam cross-section with a positioning accuracy of $\pm$ 2 mm in relation to the channel axis. The point-type counters were more convenient to use because the profiles of the beam could be measured in both transverse planes with the same counter. For investigations into the modes of operation of channel 4A, point-type counters were located behind lens unit Q4, Q5 and in the vicinity of the experimental set-up. Whenever a parallel beam was to be directed to an experimental set-up, the counters were used mainly at the stage when the beam axis was being made to coincide with the channel axis. The beam parallelism was checked with a differential Čerenkov counter. The

counting efficiency of the latter was up to 30%, which corresponds to a beam divergence of no more than $\pm$0.8 mrad. In the second case, when the beam was being focused on the experimental set-up (see the optical layout in figure 2a) the currents in the Q4, Q5 lens doublet were chosen in such a manner that the maximum count was obtained on the point-type counter, which was placed at the point where the image was formed. The beam profile was checked during this operation. The current variation in lenses Q4 and Q5 was effected by means of the following programme. For a fixed current in lens Q4, the current value in lens Q5 was found for which the point-type counter gave the maximum count. The same procedure was used for a different current value in lens Q4. The current values thus found for the Q4, Q5 lens doublet gave, when plotted, a straight line, on the basis of which all the currents in both lenses were later changed simultaneously. The measured beam profiles in the operating mode for this case are given in Figure 7a.

The same procedure was used when studying the operating modes of channel 4B, when the beam was focused on a hydrogen target placed in front of magnet M4 (see the optical layout of Figure 2b). When the beam was being formed for injection into the bubble chamber, it was necessary, in order to reduce the back-ground, to make its image coincide in the vertical and horizontal planes with the centre of collimators C6 and C7 respectively (see Figure 2b). To do this, a double-maximum method was used; it differs from that described in the literature /6/ in that the function of the pencil-type counters was, in this case, exercised by the collimators themselves. The particles in the channel were recorded only by full-flow counters placed in front and behind collimators C6 and C7. A narrow slit is installed in one of the collimators ($\pm$ 2 mm) and the other collimator is fully opened; then, for a fixed current in lens Q7 a reading is taken of the variation of the particle count when the current is altered in lens Q6. The same dependence is recorded when the slit values in the collimators are interchanged, i.e. when the collimator with the narrow slit is fully open and the slit of the

fully-open collimator is closed to $\pm$ 2 mm. The same procedure is repeated for other fixed currents in lens Q7. The points which correspond to the maximum intensities of each recorded curve are plotted on a graph with the coordinates V_6 and V_7, where V_6 and V_7 are the readings of a digital voltmeter obtained from the shunt windings of lenses Q6 and Q7 respectively (see Figure 8a). It is easy to find from the graphs of Figure 8a, the currents in lenses Q6 and Q7 at which the maximum particle intensities are obtained at the same time for both states of collimators C6 and C7, which unambiguously indicates that the particle beam images coincide with the centres of the collimators. The last lens unit, Q8 and Q9, which forms the particle beam for injection into the bubble chamber, is tuned directly according to the measurements of the beam profile. The current variation in the lenses is effected in accordance with the focal coefficients /7/. The measurements of the beam profile at the end of the channel are given in Figures 7b and c.

Tuning the first lens unit Q1, Q2 /6/ requires special treatment. This unit must form an image in the horizontal plane in the centre of the momentum collimator C4 for channels 4B and 4C, and of C5 for channel 4A. A study of the operating modes of lens Q1, Q2 was made on channel 4C. The operating mode found for lens Q1, Q2 was automatically suitable also for channel 4B (see the optical layouts in figures 2b and 2c) and was easily corrected with the focal coefficients for channel 4A. The tuning process consisted of considerably limiting the beam with the second momentum collimator C8 (see figure 2c) and, by varying the currents in lenses Q1 and Q2, of obtaining the maximum count on a counter placed at the position of the final image. The current variation sequence in lenses Q1 and Q2 was similar to that already described for the following lens units channels 4A and 4B. The dependence of the count on the current in lens Q1 is shown in figure 8b, which also gives the corresponding current variation in lens Q2. The correctness of the above procedure was checked by direct calculations of the beam profiles. The operating modes of all the lenses studied in channel 4C virtually coincided with those calculated (the difference did not exceed 1%), whilst the difference between the calculated and tuned operating conditions of lens unit Q1, Q2 was 5%. The correspondence between the calculated characteristics and the characteristics of the beams thus tuned is confirmed by direct measurements made on physics equipment. The beam profiles on the experimental installations of channel 4C when the beam was focused at a distance of 30 metres from the final lens are shown in figure 7.

The secondary particle beams in the momentum range of 25-40 GeV/c formed in the above complex meet all the requirements of the experiments carried out on them. It later proved possible to reduce the lower limit of secondary particle momenta to 20 GeV/c for an accelerated proton energy of 70 GeV. Naturally, the centres of the beams produced did not coincide with the channel axis at the accelerator exit.

The main parameters of the beams produced in the channels are given in the table. The beam dimensions in typical sections were measured for values of the aperture collimator slits suited to the requirements of the experiments. (The solid angle of particle capture in the channel was usually found to be 30% of the maximum angle).

Unlike those given in paper [1], the dimensions of the parallel beam at the end of channel 4A given in the table do not take into account the restrictions imposed by the differential Čerenkov counter.

In conclusion, the authors express their sincere thanks to R.M. Sulyaev for numerous discussions and useful comments; to Yu.D. Prokoshkin who made it possible to carry out, in the shortest possible time, the investigations into the beam characteristics and channel operating modes; and finally to all the staff responsible for servicing the accelerator, targets and channels.

Table

Beam characteristics in channels of negative particles in the 25-40 GeV/c momentum range (accelerated proton energy - 70/GeV/c, angle of particle production on the target - 0°).

Secondary particle momentum, GeV/c	40	31.6	25
Ratio of K^- meson intensity to meson flux*)	3.2×10^{-2}	4.35×10^{-2}	5.25×10^{-2}
Ratio of anti-proton intensity to meson flux	3.8×10^{-3}	6.3×10^{-3}	11.1×10^{-3}
Secondary particle intensity for $\Delta p = 1$ GeV/c with an intensity of 10^{12} protons per cycle accelerated to 70 GeV.		10^6	
Beam dimensions (channel 4A) on the experimental set-up (hor. x vert.)			
a) parallel beam		8 x 6 cm	
b) focussed beam		2.5 x 1.8 cm	
Beam dimensions on the experimental set-ups of channel 4B (hor. x vert.)			
a) on the target in front of magent M4		2 x 1.6 cm	
b) at the entrance to the bubble chamber		4 x 1.8 cm	
Beam dimensions on the experimental set-ups of channel 4C (hor. x vert.)			
a) at a focal point 30m from the final lens		3.5 x 1.6 cm	
b) at a focal point 18m from the final lens (calculated values)		0.6 x 1.4 cm	

* The relative particle yields given have been corrected for scattering and absorption and were taken from paper /8/.

References

1. I.A. Aleksandrov, M.I. Grachev, K.I. Gubrienko, E.V. Eremenko, V.I. Kotov, A.N. Nekrasov, A.A. Prilepin, V.A. Pichugin, R.A. Rzaev, A.V. Samojlov, V.S. Seleznev, B.A. Serebryakov, A.E. Khanamiryan, Yu.S. Khodyrev. IHEP Preprint 69-36, Serpukhov 1969.

2. K.I. Gubrienko, E.V. Eremenko, V.I. Kotov, A.V. Samojlov, R.M. Sulyaev, Yu.S. Khodyrev. IHEP Preprint 69-77, Serpukhov 1969.

3. A.V. Alekseev, M.D. Veselov, V.S. Kuznetsov, Yu.A. Lastochkin, I.A. Mozalevskij, A.V. Nikiforovskij, B.I. Tarasov, A.M. Frolov. IHEP Preprint 68-62, Serpukhov 1968.

4. I.A. Aleksandrov, V.P. Kartashev, A.V. Samojlov. IHEP Preprint 67-21, Serpukhov 1967.

5. I.A. Aleksandrov, V.P. Kartashev, A.V. Samojlov. IHEP Preprint 67-18, Serpukhov 1967.

6. V.I. Kotov, V.V. Miller. Focusing and mass-separation of high-energy particles. Moscow. Atomizdat 1969.

7. P. Lazeyras. CERN / D. Ph II/Beam 67-2, 1967.

8. F. Binon, S.P Denisov, P. Dyutejl', V.A. Kachanov, V.M. Kut'in, Zh.-P. Pen'e, Yu.D. Prokoshkin, A.V. Razuvaev, M. Spigel', Zh.P. Stroot, R.S. Shuvalov. IHEP Preprint 69-78. Serpukhov 1969.

Manuscript received by
Publications Group
4 November 1970.

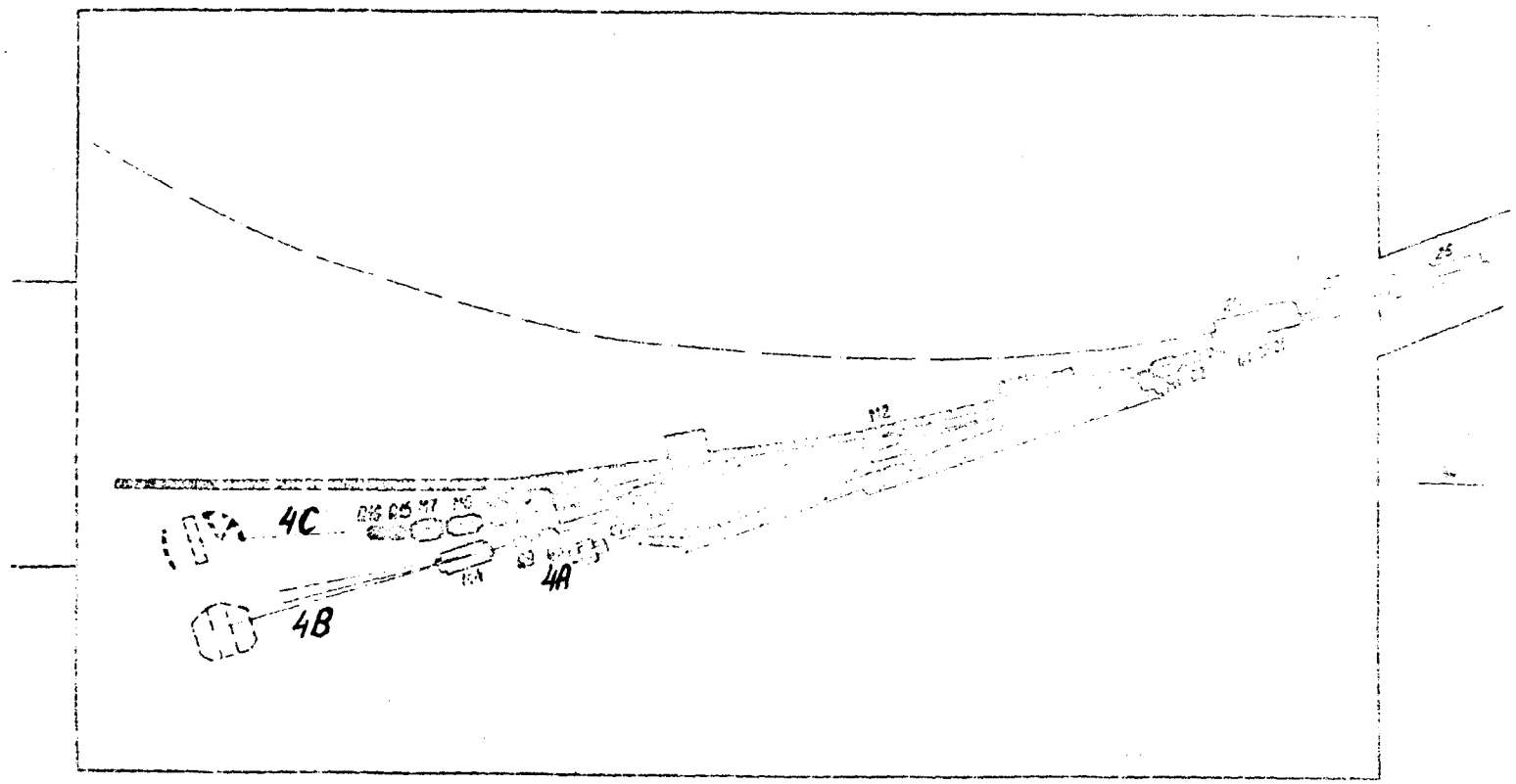

Fig. 1. Layout of channels 4A, 4B and 4C in the experimental hall.
M - bending magnets, Q - quadrupole lenses, C - collimators, T - targets.
The experimental set-ups are located in the areas bounded by the broken lines.

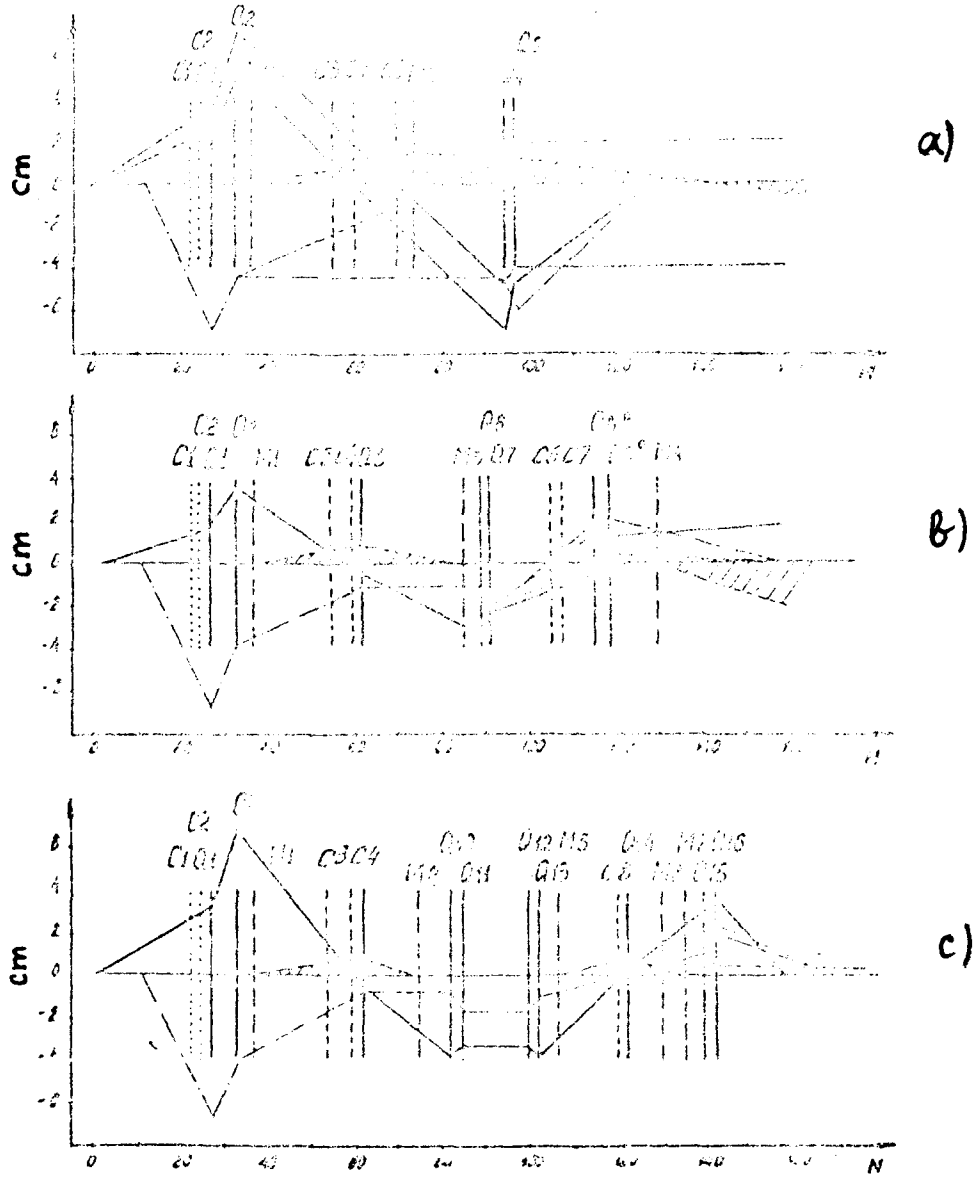

Fig. 2. Optical layouts of channels 4A - (a), 4B - (b) and 4C - (c): outer trajectories in the horizontal (————)and vertical (—— ·——) planes, dispersion curve (—— —— ——) for $P/P_o = + 1\%$.

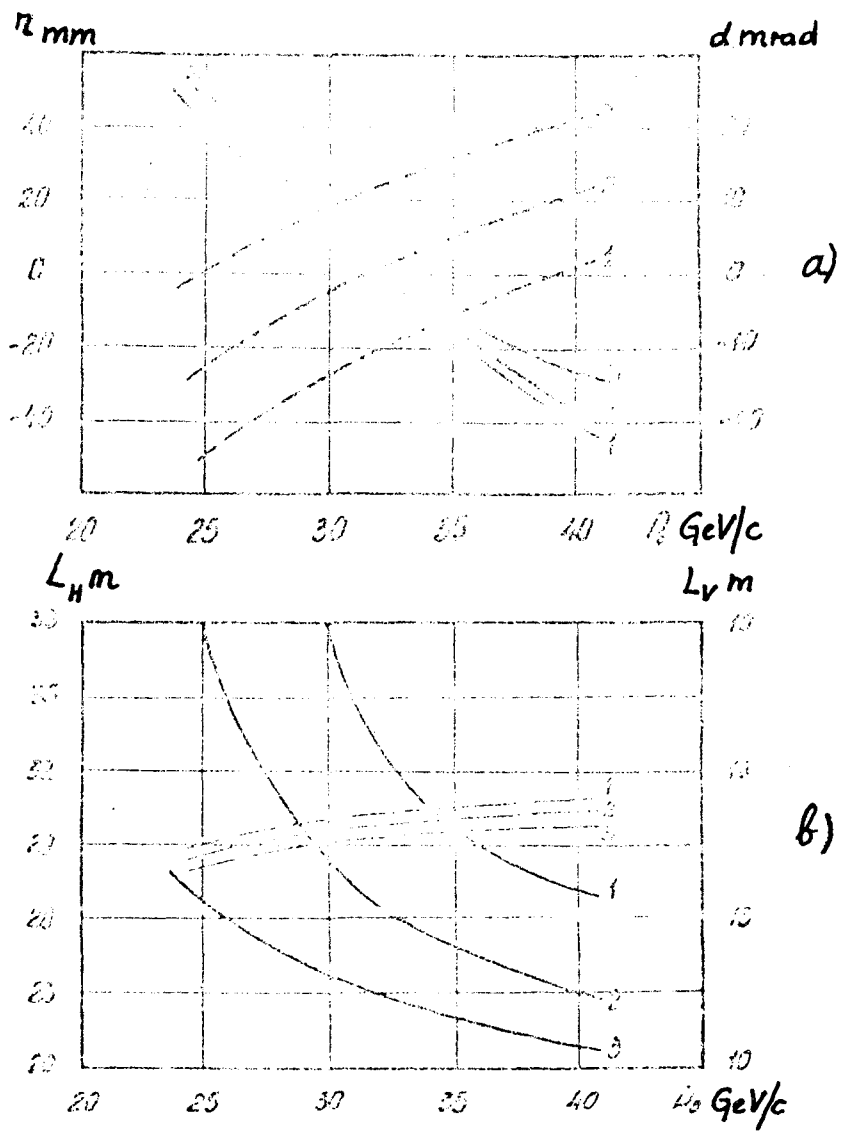

Fig. 3. Position of targets 1, 2 and 3 in relation to the equilibrium orbit (———) and secondary particle production angles (—— —— ——) as a function of their momentum - (a): distance from Q1 to the imaginary sources in the horizontal L_H (———) and vertical L_V (— . — . —) planes as a function of secondary particle momentum - (b).

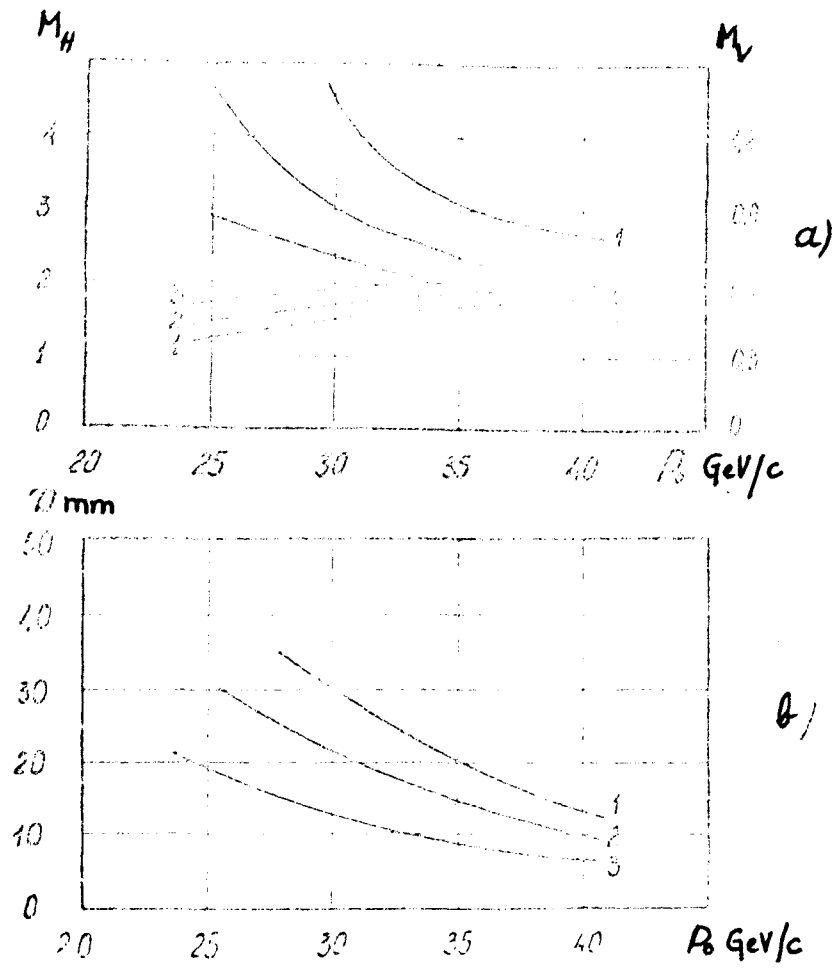

Fig. 4. Coefficients of linear magnification on the horizontal M_H (———) and vertical M_v (— . — . —) planes in the accelerator's magnetic field - (a); dispersion of imaginary sources in the horizontal plane as a function of secondary particle momentum for $\Delta p = 1$ GeV/c - (b).

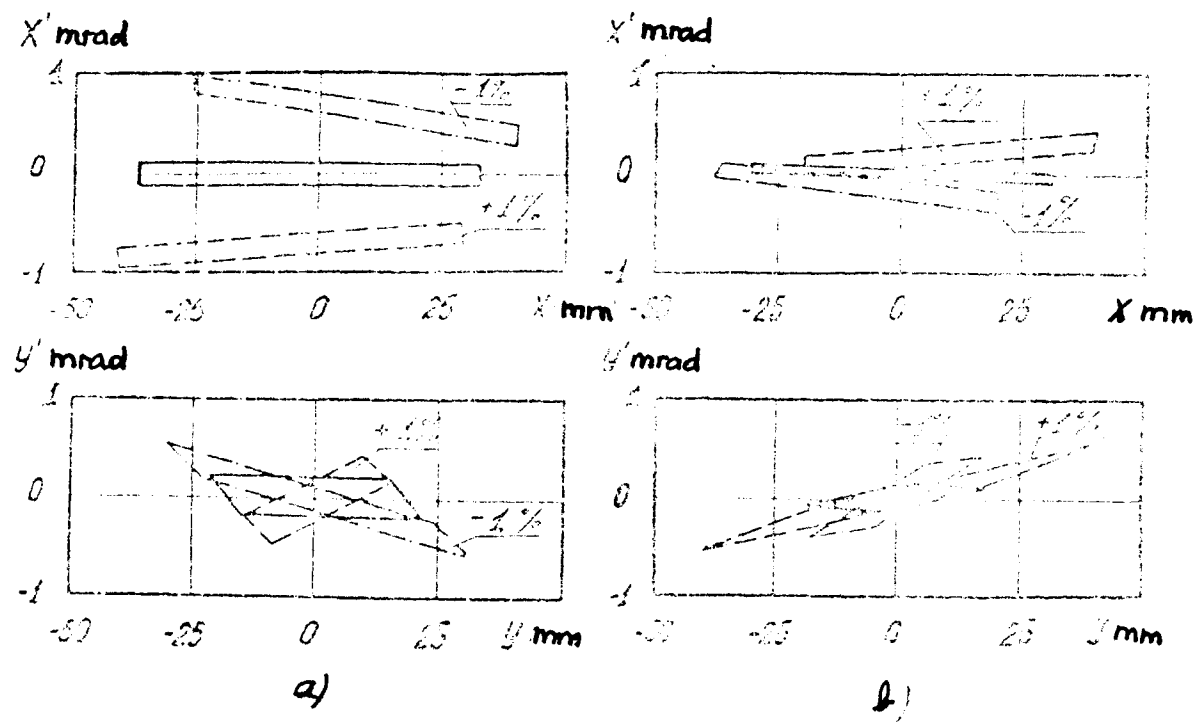

Fig. 5. Phase characteristics of the beams in the parallel sections of channels 4A (a) and 4C (b). (——) - p = p_o, (— — —) - p = 1.01 p_o, (— . —) - p = 0.99 p_o

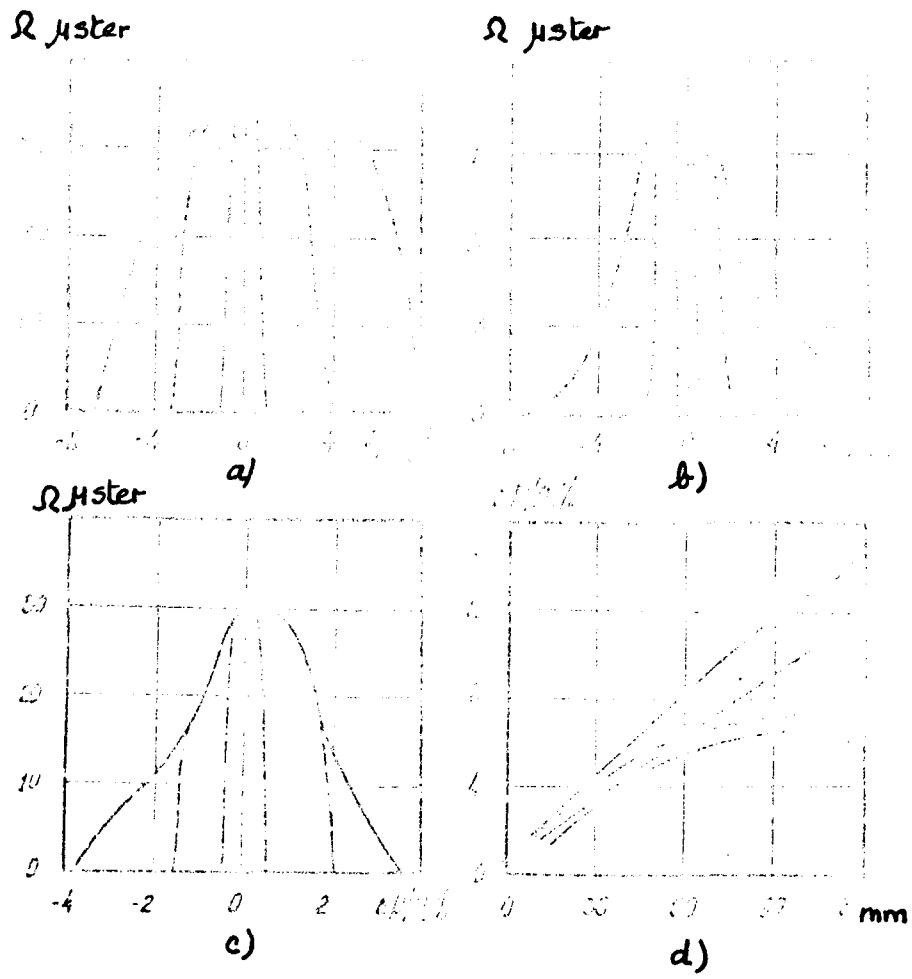

Fig. 6. Solid angles of particle capture in channels 4A - (a), 4B - (b) and 4C - (c) as a function of secondary particle momentum for various slits δ of the momentum collimators:
a) (———) - δ = 140 mm; (— — —) - δ = 60 mm; (— . —) - δ = 20 mm; b) and c) (———) - δ = 75 mm; (— — —) - δ = 25 mm; (—.—.—) - δ = 5 mm. d) is the momentum range covered as a function of the opening of the momentum collimators.
Curve 1 is for C8 (4C), Curve 2 for C4 (4C), Curve 3 for C5 (4A) and Curve 4 for C4 (4B).

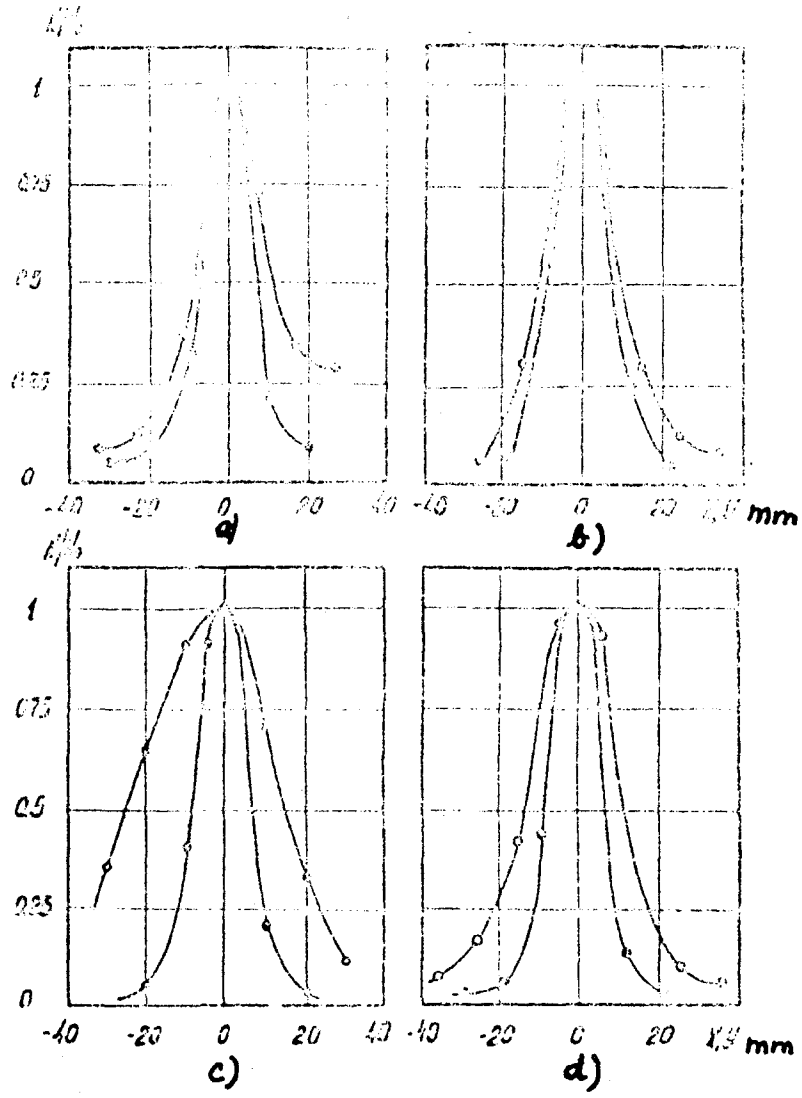

Fig. 7. Measurements of the horizontal and vertical beam profiles on the experimental set-ups of channels 4A - (a); 4B (hydrogen target) - (b); 4B (bubble chamber) - (c); and 4C (focussing at 30 m from Q16) - (d).

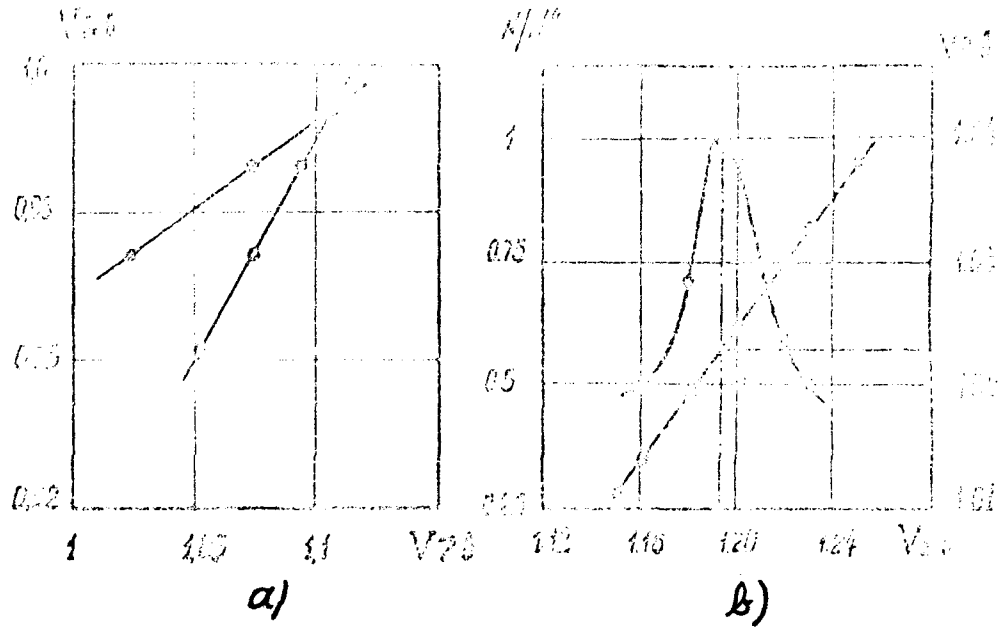

Fig. 8. Procedure for tuning lens unit Q6, Q7. (a) Lines of horizontal (—o—) and vertical (—•—) focusing. Tuning of lens unit Q1, Q2 - (b). Mutual variation of operating modes in Q1 and Q2 (—•—) and particle intensity in the channel (—o—).